

Notes

Application of a FIB–STEM system for 3D observation of a resin-embedded yeast cell

Takeo Kamino^{1,*}, Toshie Yaguchi¹, Tsuyoshi Ohnishi², Tohru Ishitani² and Masako Osumi^{3,4}

¹Hitachi Science Systems, Ltd, 11-1 Ishikawa-cho, Hitachinaka, Ibaraki 312-0057, ²Hitachi High-Technologies Corporation, 882 Ichige, Hitachinaka, Ibaraki 312-0057, ³Institute of Medical Mycology, Teikyo University, 359 Otsuka, Hachioji, Tokyo 192-0395 and ⁴Japan Women's University, 2-8-1 Mejirodai, Bunkyo-ku, Tokyo 112-8681, Japan

*To whom correspondence should be addressed. E-mail: kamino-takeo@naka.hitachi-hitec.com

Abstract The combination of a focused ion beam (FIB) system and a scanning transmission electron microscope (STEM) has been applied to the three-dimensional (3D) observation of a resin-embedded yeast cell. Using a FIB microsampling technique, a sample with a thickness of tens of micrometres was extracted from a resin-embedded block sample. The extracted sample was transferred to a FIB-STEM-compatible specimen rotation holder and trimmed by FIB milling for 3D STEM observation. Although the FIB milling was carried out at an operating voltage of 40 KV, the sample was cross sectioned without forming a harmful damage layer on its surface. Cell structures, such as cell wall, cell membrane, mitochondria, peroxisomes, endoplasmic reticulum and vacuoles, were observed clearly in a pillar-shaped sample of 20 µm long, 4 µm wide and 3 µm deep.

Keywords focused ion beam system, FIB microsampling technique, scanning transmission electron microscope, three-dimensional observation, resin-embedded yeast cell

Received 23 February 2004, accepted 3 June 2004

The focused ion beam (FIB) technique has unique and useful features in transmission electron microscope (TEM) sample preparation. First, it has less preferential sputtering than any other conventional TEM sampling method, because the Ga ion beam is used at a very low grazing angle with respect to the finally prepared TEM sample surface [1–3]. Second, the surface structure of the sample can be observed by scanning ion microscopy (SIM) and, hence, the area to be milled is located easily [4]. Recently, a dedicated FIB system for TEM sample preparation with variable operating voltages and high ion-beam current has been developed and used in the TEM investigation of various materials. In addition, a technique allowing the extraction of a sample of micrometres in size (i.e. a microsampling technique) from millimetre-sized material has been developed [5–8]. The technique has made TEM sample preparation easier and quicker, and is now applied to various materials, including those with a very low-melting point, such as toners or paraffin. However, the

FIB technique has not been applied to the TEM sample preparation of biological tissues. This is mainly because the cost of sample preparation is higher than that of the conventional ultramicrotome technique; however, the size of the sample is much smaller than that prepared by the conventional method. Recently, a technique for observing three-dimensional (3D) structures of nanomaterials has been developed. In this technique, the sample is shaped into a pillar and mounted on the tip of a needle stub, and the observation of the pillar-shaped sample is carried out using a specially designed FIB-STEM-compatible sample rotation holder. Since the technique requires the extraction of a piece of sample from a bulk sample and its shaping into a pillar, only the FIB technique can be applied.

In this study, we applied the technique to the 3D STEM observation of resin-embedded *Candida tropicalis* cells [9].

Figure 1 schematically shows the sample preparation of resin-embedded cells and their 3D observation. First, a

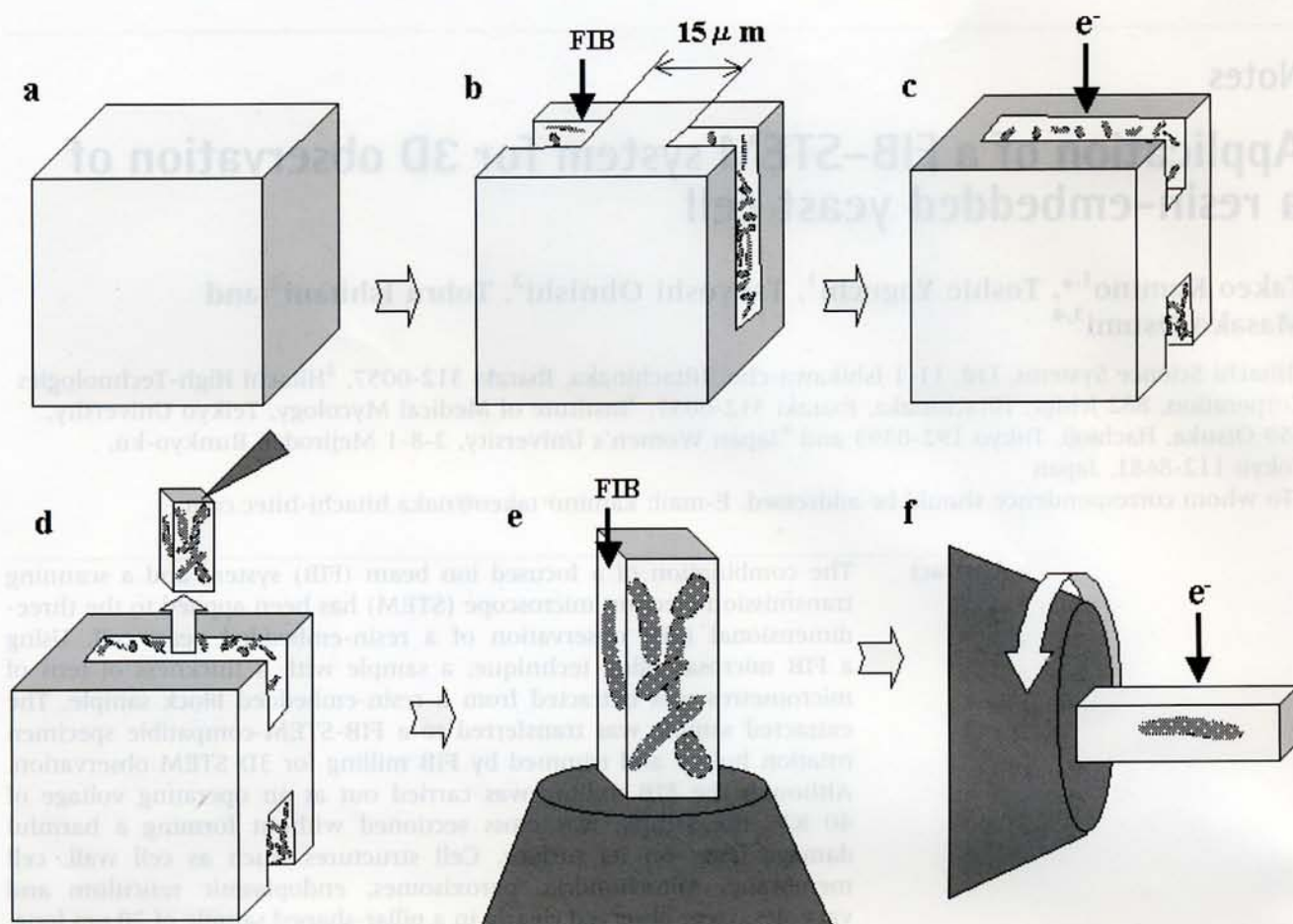


Fig. 1 Schematic flow of the FIB micropillar sampling technique. (a) Cutting out of a sub-mm-sized sample from a block sample, (b) FIB milling to a thickness of $15\ \mu\text{m}$, (c) STEM observation, (d) extracting a micropillar sample, (e) mounting the micropillar sample on a stage of a FIB-STEM-compatible sample rotation holder and trimming the sample by FIB milling, and (f) STEM observation.

sub-millimetre-sized sample was cut out from a block sample (a). Second, a part of the sample was FIB milled to a thickness of $15\ \mu\text{m}$ (b) and transferred to the STEM unit for STEM observation (c). A sample of tens of micrometres in size was extracted from the area by the FIB microsampling technique (d). The extracted sample was mounted on the sample stage of a FIB-STEM-compatible sample rotation holder and trimmed by the FIB milling technique (e), before being transferred to the STEM unit and rotated for 3D dark-field STEM observation (f).

Figure 2 shows a dark-field STEM image of a FIB cross-sectioned sample of resin-embedded *C. tropicalis* cells. The cells were fixed with 2.5% glutaraldehyde–1.5% potassium permanganate and embedded in Quetol 653 resin. Although the sample thickness is $15\ \mu\text{m}$, which is nearly 100 times greater than a standard TEM section, a number of cells are observed in various shapes and directions.

Figure 3 shows dark-field STEM images of the resin-embedded *C. tropicalis* cells observed from the front (a) and back (b) of a pillar-shaped sample, which is $15\ \mu\text{m}$ in width and depth. In the case of STEM observation of the pillar-shaped sample, the depth is the virtual thickness for



Fig. 2 Dark-field STEM image of a $15\ \mu\text{m}$ thick sample of Quetol 653 resin-embedded *C. tropicalis* cells.

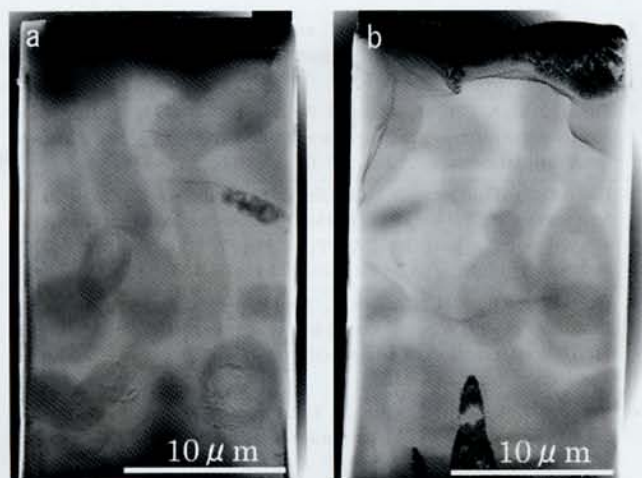


Fig. 3 Dark-field STEM images of Quetol 653 resin-embedded *C. tropicalis* cells observed from the front (a) and back (b) of a pillar-shaped sample of 15 μm in width and depth.

transmitted electrons. Since the azimuth of the observations differs by 180°, the images are mirror symmetric and the cell observed to be relatively sharp on one STEM image is blurred on the other side. As is well known, STEM image resolution is limited by the size of the incident electron beam. However, the diameter of the incident electron beam increases with the length of the path inside the sample. This is the reason why the cell observed clearly in Fig. 3a is blurred in Fig. 3b and, hence, we are able to estimate the position of the material from the clarity of the STEM image. In this study, this unique feature of STEM is utilized to locate a specific cell among a number of cells inside a thick sample. Since a conventional STEM observation can give us only two-dimensional structural information, it is difficult to judge whether the observed cell is complete or partially cross-sectioned. We therefore observed the stereoscopic STEM image prior to choosing a specific cell.

Figure 4 shows stereoscopic dark-field STEM observation of the resin-embedded *C. tropicalis* cells in a pillar-shaped sample of 9 μm wide and 7 μm deep. The azimuth difference between the two images is 10° with respect to one another. After the stereoscopic observation, the sample was transferred to the FIB system again for further trimming. Figure 5 shows stereoscopic bright-field STEM observation of the sample after the trimming into a pillar shape, 4 μm wide and 3 μm deep. Although the sample was not stained after the FIB milling, cell structures of the cell, such as cell wall (CW), cell membrane (CM), mitochondria (M) and vacuoles (V), are observed clearly and three-dimensionally in quite high contrast, as judged by our previous ultrastructural research in yeasts [9–11]. We usually stain an ultrathin sectioned specimen with uranyl acetate and lead nitrate to enhance the TEM image contrast; however, the contrast obtained in the bright-field STEM image is high enough to identify the intracellular organelles. Stereoscopic observation at higher magnification is shown in Figure 6. Beneath the cell membrane, endoplasmic reticulum (ER), regularly appearing in

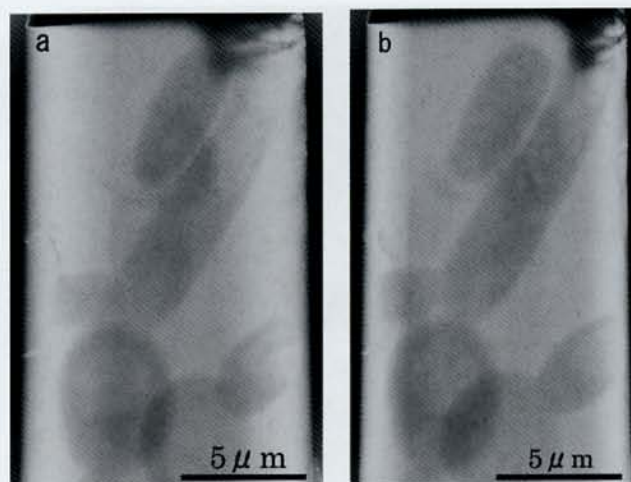


Fig. 4 Stereoscopic dark-field STEM images of Quetol 653 resin-embedded *C. tropicalis* cells in a pillar-shaped sample of 9 μm in width and 7 μm in depth. The azimuth difference between (a) and (b) is 10°.

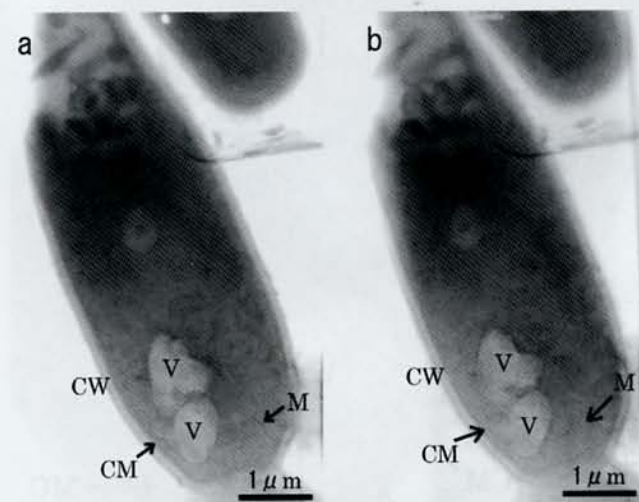


Fig. 5 Stereoscopic bright-field STEM images of Quetol 653 resin-embedded *C. tropicalis* cells in a pillar-shaped sample of 4 μm in width and 3 μm in depth. The azimuth difference between (a) and (b) is 10°. Abbreviations: CM, cell membrane; CW, cell wall; M, mitochondrion; V, vacuole.

the yeast cell [9–11] is seen. Peroxisomes (P), typical organelles in *C. tropicalis* cells grown in *n*-alkane as a sole carbon source [9], and mitochondrial cristae (MC) are identified and the 3D structure of the inside of the cell is also recognized clearly.

The surface of the sample may have been damaged by Ga-ion irradiation during the FIB milling, but no unexpected contrast is observed on the surface. The result of the experiment confirmed that the FIB technique can be used for TEM sample preparation (ultrathin sectioning) of a specific site in a resin-embedded biological tissue without any visible negative effect of the FIB milling. The STEM capability in thick sample observation also plays an important

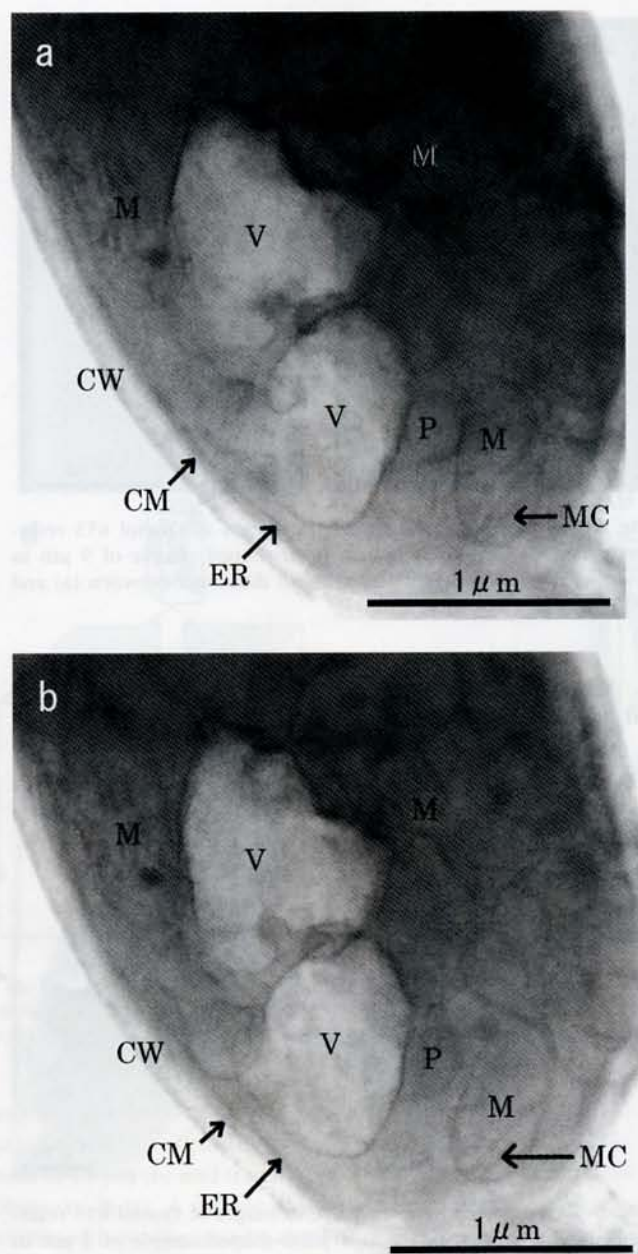


Fig. 6 High-magnification stereoscopic bright-field STEM images of Quetol 653 resin-embedded *C. tropicalis* cells in a pillar-shaped sample of 4 μm in width and 3 μm in depth. The azimuth difference between (a) and (b) is 10°. Abbreviations: CM, cell membrane; CW, cell wall; ER, endoplasmic reticulum; M, mitochondrion; MC, mitochondrial cristae; P, peroxisome; V, vacuole.

role in the proposed method. Thus, the combined use of a FIB system and a dedicated STEM unit allows us precise pin-point characterization and 3D structural study of a specific site of resin-embedded biological tissues.

References

- 1 Ishitani T, Ohnishi T, Madokoro Y, and Kawanami Y (1991) Focused-ion-beam 'cutting' and 'attacker' for micro machining and device transplantation. *J. Vac. Sci. Technol.* **B9**: 2633–2637.

- 2 Ishitani T, Tsuboi H, Yaguchi T, and Koike H (1995) Transmission electron microscope sample preparation using a focused ion beam. *J. Electron Microsc.* **44**: 331–336.
- 3 Yamaguchi A, Shibata M, and Hashinaga T (1993) Transmission electron microscopy specimen preparation technique using focused ion beam fabrication. *J. Vac. Sci. Technol.* **B10**: 575–570.
- 4 Kitano Y, Fujikawa Y, Takeshita H, Kamino T, Yaguchi T, Matsumoto H, and Koike H (1995) TEM observation of mechanically alloyed powder particles (MAPP) of Mg-Zn alloy thinned by FIB cutting technique. *J. Electron Microsc.* **44**: 376–383.
- 5 Onishi T, Koike H, Ishitani T, Tomimatsu S, Umemura K, and Kamino T (1999) A new focused-ion beam microsampling technique for TEM observation of site-specific areas. *Int. Symposium for Testing and Failure Anal.* 449–453.
- 6 Kamino T, Yaguchi T, Ohnishi T, Umemura K, and Tomimatsu S (2000) Site specific TEM preparation using an FIB/STEM system. *Microsc. Microanal.* **6**: 510–511.
- 7 Yaguchi T, Kuroda Y, Ueki Y, Kamino T, Ohnishi T, Umemura K, and Asayama K (2002) Three dimensional characterization of a specific site by an FIB microsampling technique. *Microsc. Microanal.* **7**: 938–939.
- 8 Kamino T, Yaguchi T, Kuroda Y, Hashimoto T, Ohnishi T, Ishitani T, Umemura K, and Asayama K (2002) Development of a dedicated FIB system and its application. *Microsc. Microanal.* **8**: 48–49.
- 9 Kamasawa N, Naito N, Kurihara T, Kamada Y, Ueda M, Tanaka A, and Osumi M (1996) Immunoelectron microscopic observation of behaviors of peroxisomal enzymes inducibly synthesized in an *n*-alkane-utilizable yeast cell *Candida tropicalis*. *Cell Struct. Funct.* **21**: 117–122.
- 10 Osumi M, Miwa N, Teranishi Y, Tanaka A, and Fukui S (1974) Ultrastructure of *Candida* yeasts grown on *n*-alkanes—appearance of microbodies and their relationship to high catalase activity. *Arch. Microbiol.* **99**: 181–201.
- 11 Osumi M (1998) The ultrastructure of yeast: cell wall structure and formation. *Micron* **29**: 207–233.